Royal Netherlands
Meteorological Institute
Ministry of Infrastructure
and Water Management

PGV levels and location uncertainty for the Emlichheim 13-08-2024 event

E. Ruigrok and L. Evers

De Bilt, 2024| Technical report; TR 24-5

Royal Netherlands
Meteorological Institute
Ministry of Infrastructure
and Water Management

PGV levels and location uncertainty for the Emlichheim 13-08-2024 event

KNMI, R&D Seismology and Acoustics

September 28, 2024

Introduction

The Emlichheim event on 13-08-2024:22:51:30.4 with a local magnitude of 1.81 was detected by the KNMI network (*KNMI*, 1993) and located near-real time with the Hypocenter method (*Lienert et al.*, 1986). This fast solution uses an average 1D model for the north of the Netherlands (*Kraaijpoel and Dost*, 2013). In this report, an updated location and its uncertainty is derived. Moreover, peak-ground velocity (PGV) levels are extracted from the recordings. These are used, together with a ground motion prediction equation, to find out where PGV levels of 2 mm/s and higher may have occurred.

Epicenter

The epicenter is improved by using a best-fitting traveltime versus distance model based on a database of local P-wave traveltime picks. This data-driven model incorporates actual underburden velocities and only well pickable phase arrivals. An error estimate is derived from the spread in picking times from the best-fitting model. This error incorporates both the local variations of the velocity field as well as picking errors. These errors are propagated further into the epicentral probability density function (PDF). This results into an updated epicenter and its 95% confidence region. Details of the method are described in *Ruigrok et al.* (2023).

Fig. 1 shows the seismic sensors where manual P-wave picks are available. The event is well covered with Dutch stations north, west and south of the event. We have no access to data from German stations within 50 km distance from the event. Using the indicated Dutch stations, a grid search is performed for a region around the Hypocenter solution, as indicated by the red boxes in the figure. In the first step, equal differential time (EDT, *Zhou*, 1994) residuals are computed. That is, for each grid point and for each station combination, the traveltime differences are forward modelled and tabulated. From these values, the observed traveltime differences are subtracted to obtain the EDT residuals. In the second step, the PDF is derived from the EDT residuals, using a L1 norm (*Tarantola*, 2005). Fig. 2 shows the 95% confidence area of the resulting PDF. The locations with the maximum probability is assigned to be the updated epicenter.

The following list contains the new epicenter for the Emlichheim 13-08-2024 event, both in wgs84 coordinates and in the Dutch national triangulation system (RD). The line that surrounds the 95% confidence zone is by approximation an ellipse. The parameters of this ellipse (major axis, minor axis and orientation) are listed, together with the standard deviations describing the epicentral PDF in the direction with the largest uncertainty σ_1 and the perpendicular direction with the smallest uncertainty σ_2.

Epicenter in wgs84 [deg]: 6.8529, 52.6418
Epicenter in RD [m]: 254200, 518150
Ellipse major and minor axes [m]: 1286, 1153
σ_1 and σ_2 [m]: 263, 236
Orientation of the major axis [deg]: 72

The waveform data used in the above analysis is publicly available and can be obtained through:

GUI: `http://rdsa.knmi.nl/dataportal/`

FDSN webservices: `http://rdsa.knmi.nl/fdsnws/dataselect/1/`

Relative location

The event described in this report is similar to a M2.14 event on 13-03-2024 that is discussed in *Ruigrok et al.* (2024). For the March event, a depth analysis was done pointing to a depth between 3 and 5.5 km. In this depth range the Schoonebeek gasfield exists, which was found to be the most likely source for the event. The depth was fixed at the gas-water contact, which is at 3.3 km depth.

The location for both Emlichheim events is very similar. In fact, with the Hypocenter method (*Lienert et al.*, 1986) both events were placed at exactly the same location. Using a local travel-time model (as in the previous section) the August event is found at 290 m north of the March event. The distance between the events is smaller than the 95% confidence zone, which makes it uncertain what the actual relative orientation is between the two events. Given a large similarity of waveforms, both events likely originated at the same fault and cross-correlations can be used to find the difference of S-wave minus P-wave delay times between the two sources. We estimated the S-P delay-time differences for a set of stations covering different azimuths (L2087, SNB, COE2,VBG4 and T084) and inverted for the likely relative location of both events using the same approach as in *Jagt et al.* (2017). In this approach, the assumption is made that the delay times are caused by a horizontal distance of the events. With this assumption, we find that the August event is about 140 m northwest of the March event.

The S-P delay-time differences are 0.03 s or less. This means that also the depth of the August event must be within a two-hundred meters of the March event. In the following we assume that also the August event occured at 3.3 km depth.

PGV levels

For induced events outside Groningen, the protocol as established in *Ruigrok and Dost* (2020) is used to compute PGV[1] contours. From the spatial distribution of PGV, contours are extracted for the P50, P90 and P99 probabilities. The P50 is the average field, which thus has a 50% probability of exceedance. The P90 is the 90th percentile, which PGV field has a 10% probability of exceedance. The P99 has a 1% probability of exceedance.

The PGV field is a combination of a model and local recordings. The model BMR2 (*Ruigrok and Dost*, 2020) is used. This is a ground motion prediction equation that provides the PGV level and its variability as a function of magnitude, epicentral distance and depth of the event. The model has been calibrated with PGV recordings from induced events in the Netherlands. Recordings at the Earth's surface from one specific event are used to estimate how much stronger, or weaker, this event is with respect to the average event in the database. This yields the so-called event

[1] In this report, as PGV measure we use 'PGVrot', which is defined as $max(\sqrt{u_E^2(t) + u_N^2(t)})$, where $u_E(t)$ and $u_N(t)$ are the particle-velocity recording on the East and North component, respectively.

term, which is used to adapt the model with a distance-independent shift up-, or downwards. Still, uncertainty exists of the actual PGV that materialized at a certain location. This so-called within-event variability is caused, e.g., by the radiation pattern of the source and variations in near-surface amplification. At and nearby places where the PGV has been recorded, the uncertainty of the PGV is reduced by blending the model with the actually measured PGV. If the combined field reaches levels of 2 mm/s and higher, PGV contours are extracted and shown on a map.

All accelerometer recordings at distances smaller than 50 km are evaluated, which yields 15 recordings with a signal-to-noise ratio larger or equal to 6 dB. The nearest and furthest accepted stations are at 4.89 and 48.36 km epicentral distance, respectively. Table 1 lists the PGV values, with the largest value being 0.113 mm/s. Fig. 3 shows these recorded PGV values as function of epicentral distance, together with the event-term shifted BMR2 model for M=1.81 and an event depth of 3.3 km.

Using the 15 recordings results in an event term of -0.053. This is the average difference between recorded and modeled PGV levels (expressed in natural log). With the event term quantified, the remaining model variability is the within-event variability $\phi = 0.536$. This remaining variability is implemented to yield the confidence regions as plotted in Fig. 3. This figure shows that the P50 and P90 fields do not reach the 2 mm/s threshold level, but the P99 field does.

The radially-symmetrical PGV fields (Fig. 3) are locally corrected with the recorded PGV levels (Table 1) to obtain estimates of the PGV distribution over the Earth's surface. For the P99 field (1% chance of exceedance) an area remains where the 2 mm/s threshold level is exceeded (Fig. 4). The gridded versions of the contours are available as kml files.

Station name	**Epicentral distance [km]**	**PGV [mm/s]**
SNB	4.89	0.113
COE2	9.98	0.042
OOTH	11.84	0.047
COE3	13.89	0.095
HRDB	16.94	0.040
LUTT	19.26	0.012
T020	21.60	0.009
T030	23.95	0.013
T050	29.28	0.008
T080	29.72	0.009
T060	33.43	0.011
ELE	39.61	0.010
DR030	46.39	0.003
VRS	46.91	0.008
WSVN	48.36	0.014

Table 1: Recorded PGVs

Discussion and Conclusions

The epicenter of the M1.8 Emlichheim earthquake is in Germany, approximately 1 km south of the Dutch-German border. It is located within two-hundred meters northwest of the M2.1 Emlichheim event that occured on 24-03-2024. Also the depth difference is within two-hundred meters. Since the 24-03-2024 event likely originated at the Schoonebeek gasfield, also the 13-08-2024 event likely originated at the same fault in that gasfield.

The highest recorded PGV is 0.113 mm/s at station SNB. A ground-motion prediction equation and the measured PGV values have been used to compute the PGV fields that have a 50%, a 10% and a 1% chance of exceedance. Fixing the source depth at 3.3 km, the P50 and P90 fields stays below 2 mm/s and the P99 field reaches levels between 2 and 3 mm/s in the epicentral area.

References

Jagt, L., E. Ruigrok, and H. Paulssen (2017), Relocation of clustered earthquakes in the Groningen gas field, *Netherlands Journal of Geosciences*, *96*(5), s163–s173, doi:10.1017/njg.2017.12.

KNMI (1993), Netherlands Seismic and Acoustic Network, Royal Netherlands Meteorological Institute (KNMI), Other/Seismic Network, `https://doi.org/10.21944/e970fd34-23b9-3411-b366-e4f72877d2c5`.

Kraaijpoel, D., and B. Dost (2013), Implications of salt-related propagation and mode conversion effects on the analysis of induced seismicity, *Journal of Seismology*, *17*(1), 95–107.

Lienert, B. R., E. Berg, and L. N. Frazer (1986), HYPOCENTER: An earthquake location method using centered, scaled, and adaptively damped least squares, *Bulletin of the Seismological Society of America*, *76*(3), 771–783.

Ruigrok, E., and B. Dost (2020), Advice on the computation of peak-ground-velocity confidence regions for events in gas fields other than the Groningen gas field, *KNMI Technical Report*, *TR-386*, `https://cdn.knmi.nl/knmi/pdf/bibliotheek/knmipubTR/TR386.pdf`.

Ruigrok, E., P. Kruiver, and B. Dost (2023), Construction of earthquake location uncertainty maps for the Netherlands, *KNMI Technical Report*, *TR-405*, `https://cdn.knmi.nl/knmi/pdf/bibliotheek/knmipubTR/TR405.pdf`.

Ruigrok, E., J. Spetzler, and P. Kruiver (2024), PGV levels and location uncertainty for the Emlichheim 24-03-2024 event, *KNMI Technical Report*, *TR 24-02*, `https://www.knmi.nl/research/publications/pgv-levels-and-location-uncertainty-for-the-emlichheim-24-03-2024-event`.

Tarantola, A. (2005), *Inverse Problem Theory and Methods for Model Parameter Estimation*, SIAM, Philadelphia.

Zhou, H.-w. (1994), Rapid three-dimensional hypocentral determination using a master station method, *Journal of Geophysical Research: Solid Earth*, *99*(B8), 15,439–15,455.

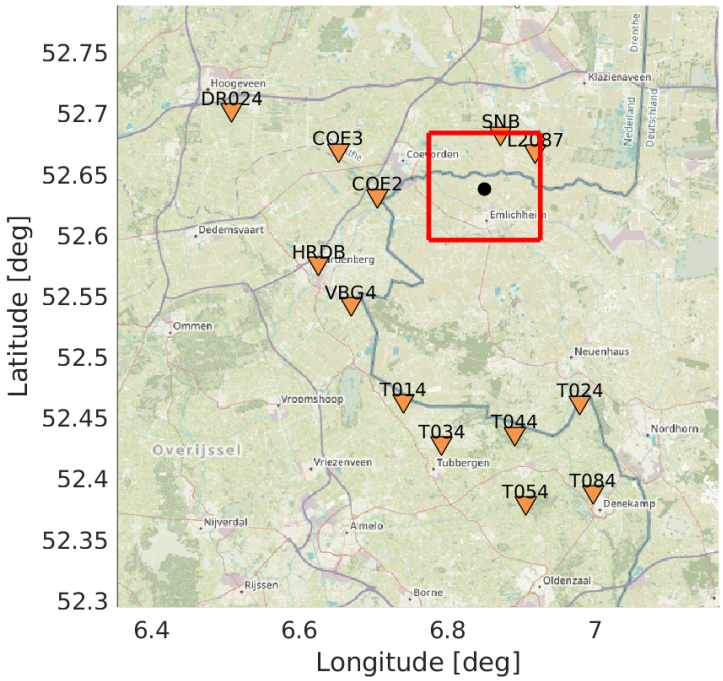

Figure 1: Overview map with locations of stations (orange triangles) where P-wave onsets were picked, the fast Hypocenter solution (black dot) and the boundary line of the area in which a grid search is done (red box). Background map is from www.openstreetmap.org.

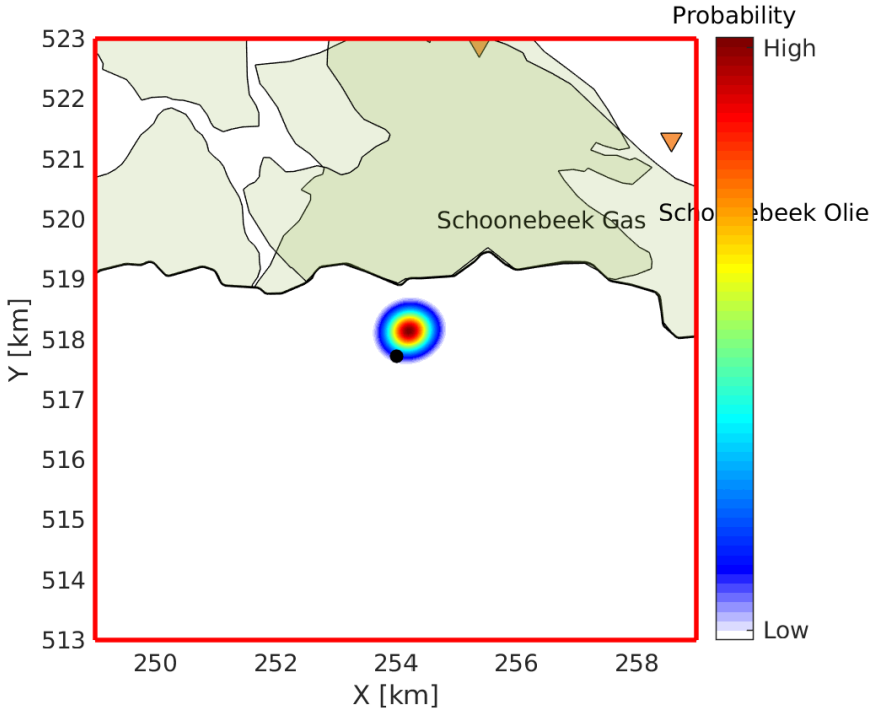

Figure 2: Map showing hydrocarbon fields (green-filled polygons), the fast Hypocenter solution (black dot) and the epicentral probability density function (PDF) using time-differences and an optimized model. The 95% confidence area of the PDF is shown. The field polygons are from www.nlog.nl, using the March 2023 update. The extension of the fields to the German side of the border is not shown.

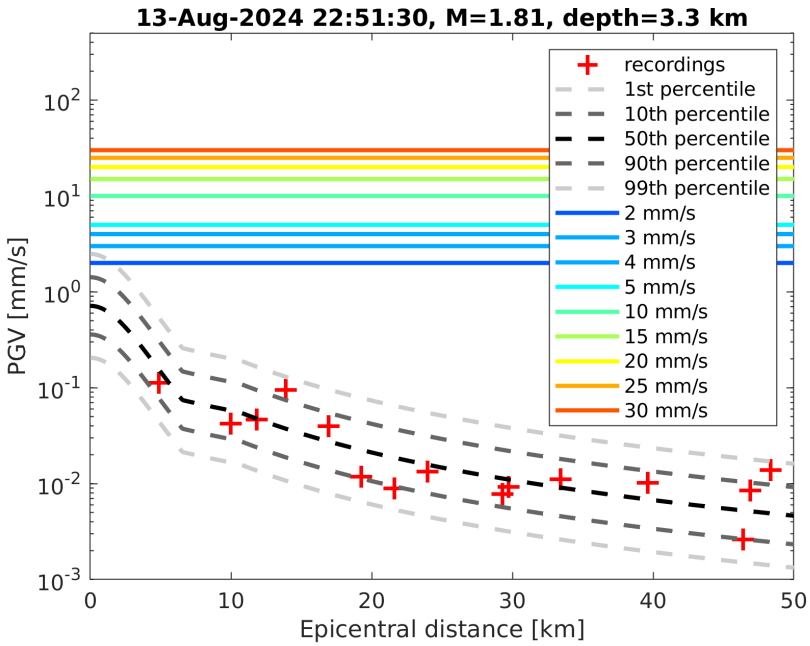

Figure 3: BMR2 model and confidence regions for this model (dashed lines), PGV thresholds (coloured lines) and measured PGV values for the Emlichheim event (red crosses). Both the model and the recordings are expressed in PGVrot.

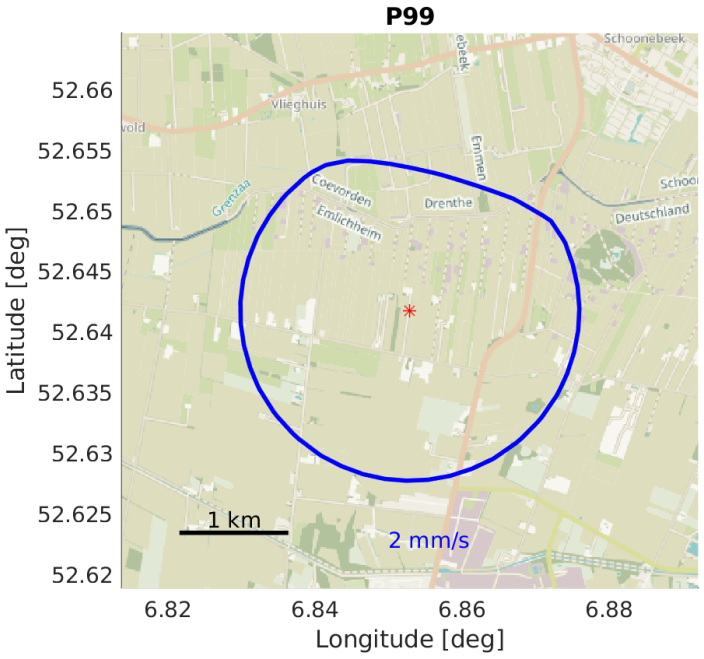

Figure 4: The bounding line of the 2 mm/s PGV threshold regions for the P99 model, and the updated epicenter (red star).

Royal Netherlands Meteorological Institute

PO Box 201 | NL-3730 AE De Bilt
Netherlands | www.knmi.nl